Laser-based diagnostics applications for plasma-surface interaction studies

2013 JINST 8 C11011

(http://iopscience.iop.org/1748-0221/8/11/C11011)

PUBLISHED BY IOP PUBLISHING FOR SISSA MEDIALAB

RECEIVED: *September 16, 2013*
ACCEPTED: *October 21, 2013*
PUBLISHED: *November 15, 2013*

16th INTERNATIONAL SYMPOSIUM ON LASER-AIDED PLASMA DIAGNOSTICS,
22–26 SEPTEMBER 2013,
MADISON, WISCONSIN, U.S.A.

2013 JINST 8 C11011

Laser-based diagnostics applications for plasma-surface interaction studies

H.J. van der Meiden,[a,1] M. A. van den Berg,[a] S. Brons,[a] H. Ding,[b] H.J.N. van Eck,[a] M.H.J. 't Hoen,[a] J. Karhunen,[d] T.M. de Kruif,[a] M. Laan,[c] C. Li,[b] A. Lissovski,[c] T.W. Morgan,[a] P. Paris,[c] K. Piip,[c] M.J. van de Pol,[a] R. Scannell,[e] J. Scholten,[a] P.H.M. Smeets,[a] C. Spork,[a] P.A. Zeijlmans van Emmichoven,[a] R. Zoomers[a] and G. De Temmerman[a]

[a] *FOM Institute DIFFER, Dutch Institute for Fundamental Energy Research, Association EURATOM-FOM, Trilateral Euregio Cluster, P.O. Box 1207, 3430 BE Nieuwegein, The Netherlands*

[b] *School of Physics and Optical Engineering, Key Laboratory of Materials Modification by Laser, Ion and Electron Beams, Chinese Ministry of Education, Dalian University of Technology, Dalian 116024, PR China*

[c] *Institute of Physics, University of Tartu, Association Euratom-Tekes, Tahe 4, Tartu 51010, Estonia*

[d] *VTT, Association Euratom-Tekes, PO Box 1000, 02044 VTT, Finland*

[e] *EURATOM/CCFE Fusion Association, Culham Science Centre, Abingdon, Oxfordshire, OX14 3DB, United Kingdom*

E-mail: h.j.vanderMeiden@differ.nl

[1] Corresponding author.

doi:10.1088/1748-0221/8/11/C11011

ABSTRACT: Several laser based diagnostics are implemented on to the linear plasma generator Magnum-PSI, wherein ITER divertor relevant plasma-wall conditions are realized. Laser Induced Desorption Quadrupole Mass Spectroscopy (LID-QMS) and Laser Induced Breakdown Spectroscopy (LIBS) are installed to measure deuterium retention in plasma facing components. Combined with Thermal Desorption Spectroscopy, LID-QMS can be used to measure lateral retention profiles. LIBS is used to measure the surface composition qualitatively, after plasma exposure. An advanced Thomson Scattering (TS) system measures electron density, neutral density and electron temperature profiles (spatial resolution < 2 mm) across the maximum 100 mm plasma diameter. Very low electron density (9×10^{18} m^{-3}) can be measured within seconds with accuracies better than 6%. The minimum measurable electron density and temperature are $\sim 1 \times 10^{17}$ m^{-3} and ~ 0.07 eV, respectively. By virtue of the high system sensitivity, single pulse TS can be performed on high density pulsed plasmas (used for replicating ELMs). For measuring the ion temperature and flow velocity of the plasma a Collective TS system (CTS) is being built: the small Debye length of the Magnum-PSI plasma enables application of this method at relatively short laser wavelength. In a feasibility study it was shown that forward CTS with a seeded Nd:YAG laser operating at 1064 nm, can be applied at Magnum-PSI to measure ion temperature and axial velocity with an accuracy of $< 8\%$ and $< 15\%$, respectively. Two high spectral resolution (~ 0.005 nm) detection schemes are applied simultaneously: an Echelle grating spectrometer (enabling profile measurements) and a system based on a Fabry-Perot etalon that enables wavelength scanning over its free spectral range, by tilting the device. The status and performance of the various laser based plasma and surface diagnostics will be reported along with experimental results.

KEYWORDS: Plasma diagnostics - charged-particle spectroscopy; Plasma diagnostics - interferometry, spectroscopy and imaging

2013 JINST 8 C11011

Contents

1 Introduction

The tokamak ITER [1] is presently under construction and aims at producing 10 times more fusion power than the external heating power. Control of the heat load on plasma facing components inside the divertor is essential for reliable tokamak operation. For predictions of divertor operation under those conditions, plasma and neutral models with radiation transport and particle trapping need to be validated with high-quality data. To get a clear understanding of the plasma surface interaction under those conditions one needs a good characterization of the surface and of the plasma. The high flux linear plasma generator Magnum-PSI [2] can play a critical role in this respect as it mimics high plasma power fluxes ($> 10\,\mathrm{MW/m^2}$) and utilizes an excellent diagnostic access. In order to simulate Edge Localized Modes (ELMs) Magnum-PSI can produce repetitive transient power loads of $1\,\mathrm{GW/m^2}$ (1 ms) by operating the plasma source in pulsed mode.

A wall-stabilized cascaded arc produces a 100 mm diameter hydrogen, argon or helium plasma jet [3, 4]; it can be operated continuously or in pulsed mode [5]. The electron density and temperature of the plasma can reach values above $5.0 \times 10^{21}\,\mathrm{m^{-3}}$ and 5 eV, respectively. The plasma jet is confined by an axial magnetic field ($< 1.9\,\mathrm{T}$) and is transported over a distance of about 1.5 m to a target. Three roots blower stages (total pump capacity $52500\,\mathrm{m^3/hr}$) are implemented and a skimmer between source and target chamber allows for differential pumping; this is necessary to maintain a low ambient pressure ($\sim 1\,\mathrm{Pa}$) in the target chamber during high particle and energy flux generation [6].

In this paper, laser based diagnostics are described that are being used or developed at Magnum-PSI. Besides optical emission spectroscopy for measuring the plasma composition and plasma velocity, a fast visible light camera (equipped with band pass filters) and a fast infrared (IR

2013 JINST 8 C11011

camera) are used for observation of the near surface plasma and the temperature of target surface, respectively. An advanced incoherent Thomson scattering (TS) system is operated routinely and is used as a control tool for the plasma conditions by measuring electron density (n_e) and temperature (T_e) profiles [7]. For unambiguous determination of ion temperature and plasma velocity a collective Thomson scattering system is under construction [8]. It will be first implemented on the linear plasma generator Pilot-PSI [9], the forerunner of Magnum-PSI. Plasma velocity and plasma temperature parameters are not only important for determination of the particle flux to the target, but also for understanding plasma heating and recombination mechanisms — which is crucial to understand plasma detachment.

Laser Induced Desorption Quadrupole Mass Spectroscopy (LID-QMS) [10] and Laser Induced Breakdown Spectroscopy (LIBS) [11] are installed to measure deuterium retention and surface composition on plasma facing surfaces. Combined with Thermal Desorption Spectroscopy, LID-QMS can be used to measure lateral retention profiles. LIBS enables measurements of depth profiles and surface composition (qualitatively), i.e. surface modifications can be measured due to plasma exposures.

A general overview of Magnum-PSI and the infrastructure for the purpose of diagnostics is given in section 2. The laser based diagnostics TS, CTS, LIBS and LID-QMS are described in section 3 including some typical results. For CTS, only the anticipated performance will be given because the system is still being constructed. The report is finalized with a summary and discussion in section 4.

2 Magnum-PSI and infrastructure for diagnostics

The central part of Magnum-PSI consists of the source chamber (SC, vessel diameter 600 mm), on which the cascaded arc plasma source is mounted, and the target chamber (TC, vessel diameter 500 mm) that hosts the target during plasma exposure (see figure 1). The produced plasma is confined by an axial magnetic field (< 1.9 T) and is transported to the target. A target manipulator is used for moving the targets of interest over a distance of about 5 m from the target chamber to the target exchange and analysis chamber (TEAC) maintaining vacuum conditions to preserve target surface conditions.

The laser beam lines for TS reach the source and the target chamber through the lower diagnostic ports in the vessel. LIBS and LID-QMS are applied inside the TEAC for surface analysis after plasma exposure. The laser beam line for LIBS is based on a conventional beam line while that for LID-QMS is fiber based. The laser room and the Magnum-PSI machine are located in different parts of the laboratory, making laser beam lines as long as 36 m necessary.

3 Laser based diagnostics

3.1 Incoherent Thomson scattering system

For maintenance purposes, the magnet of Magnum-PSI is mounted on a rail system that allows for a translation along its axis. In case the magnet has to be translated, laser injection and dump tubes that penetrate the magnet (see figure 2) have to be removed within a few hours. Moreover, coupling

2013 JINST 8 C11011

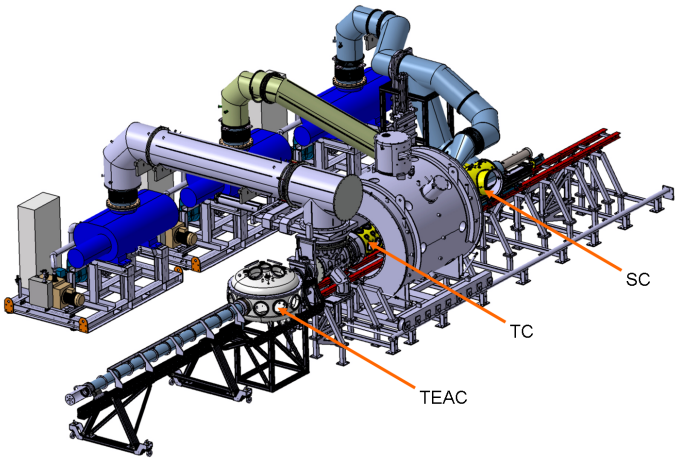

Figure 1. Schematic view of Magnum-PSI. An axial magnetic field confines the plasma until it impinges on a target. During plasma exposure, the target is located in the target chamber (TC). After plasma exposure, a manipulator arm transports the target to the target exchange and analysis chamber (TEAC) to perform detailed ex-situ analysis of the target.

and decoupling of the tubes have to be done from outside the magnet. The system is designed such that it complies to these specifications.

TS can be performed at two locations [7]. First, close to the cascaded arc output, to determine the plasma conditions before the actual exposure (in which case a plasma dump is inserted between source and target). Secondly, just in front of the target, to measure the plasma conditions during plasma exposure.

To allow for quasi real time monitoring of the plasma jet conditions, the TS system provides T_e and n_e profiles with a repetition period of 1 second. The fastest repetition period (200 ms, determined by camera read-out speed) can be achieved during single pulse TS.

The TS system is equipped with a Spectron laser, model SL 8354 and is installed in the laser room. The laser delivers 0.7 J/pulse (diameter 9.5 mm) at the second harmonic (532 nm) at 10 Hz repetition rate (beam divergence 0.5 mrad, full angle pointing stability 17 μrad). After passing a beam expander ($M = 3$) the resulting 38 mm diameter laser beam is guided from the laser room to the Magnum-PSI vessel by multilayer mirrors. After mirrors M3 and M5 (see figure 2), 3.2 m plano-convex lenses are installed to focus the beam to a spot size of about 0.5 mm at the plasma centre. After passing the plasma, the beam (as well as stray light) is dumped via a top mirror on a laser dump, located at about 240 cm above the plasma centre. Mirror M3 is controlled by a pneumatic actuator to enable TS in source and target chamber in an alternating way (switching period a few seconds). The laser beam line is remotely controlled by mirror units equipped with piezo-based actuators (PZA12, Newport).

For each TS location, the TS light originating from the corresponding laser chord is imaged onto a fiber array by a viewing system (see left insert of figure 2). At the target location, a lens (Nikkor 85 mm $f/1.8$) images the 95 mm long laser chord onto a linear fiber array of 59 fibers (40 m length, 26.7 mm input height, array format 59×1; CeramOptek UV400/424P). The viewing system at the source chamber has the same magnification ($M = 0.267$) as that of the viewing system

2013 JINST 8 C11011

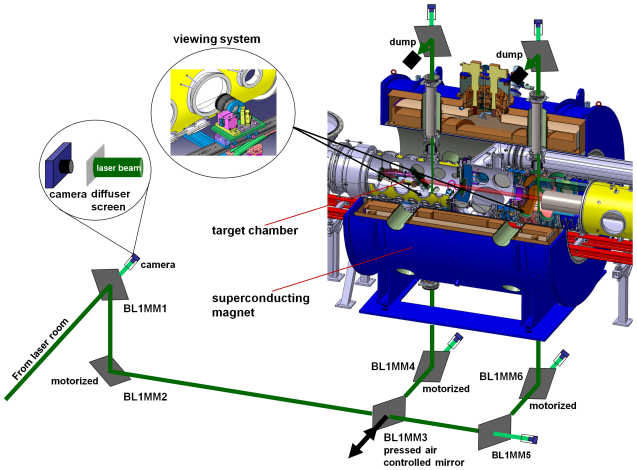

Figure 2. The 34 m long TS laser beam line together with the target chamber and source chamber of Magnum-PSI. The laser beam alignment is monitored by simple non-synchronizes CMOS cameras and controlled by mirror mounts equipped with piezo-based actuators.

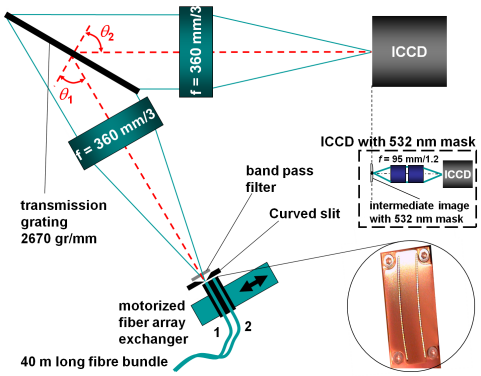

Figure 3. Schematic top view of the spectrometer. A fiber exchanger enables selection between TS in front of the target and close to the plasma source. In case the viewing dump is non-functional, an intermediate image with a 532 nm blocking strip can be applied.

used at the target chamber making use of another lens (Nikkor 135 mm $f/2$). For both locations, the spatial resolution in the plasma is about 2 mm and the viewing f-number is larger than $f/11$. The TS light collected by the viewing systems is relayed by the fiber bundles to the input of a transmission grating spectrometer. This spectrometer [12] features a high etendue (with f-number of $f/3$) and high wavelength dispersion. The required fiber array is selected by a motorized fiber array exchanger (see figure 3), combined with an entrance slit ($25 \times 0.6\,\mathrm{mm}^2$).

Transmission gratings with different groove frequencies can be used (see table 1), enabling a measurement range of ~ 10.2 nm and ~ 17.9 nm centered around 532 nm: this enables temperature measurements of more than 11 eV and 34 eV, respectively. Depending on the chosen spectral range the incident angle θ_1 and diffraction angle θ_2 are both about 45° and 61° (see figure 3).

The dispersed TS light is imaged onto the photocathode of the PI-max 1300 ICCD camera. The 25 mm diameter Generation III image intensifier is fiber optically coupled to a front-illuminated CCD (1340×1300 pixels, pixel size 20 μm square, ADC 16-bit).

A gate window of 25 ns is applied to catch the TS photons originating from the 12 ns (FWHM) laser pulse, making the plasma light background insignificant. To minimize the stray light originating from the opposite vessel walls, viewing dumps are installed at the side opposing the viewing systems. In addition, the stray light originating from the output window is reduced by a factor 2 by switching the image intensifier gate window off, just before the stray light arrives.

A good demonstration of the sensitivity of the system can be found in [7]; the expansion of a non-magnetized argon plasma was explored by Rayleigh (RS)-TS [13]. TS profiles of T_e, n_e and neutral density (n_0) were measured in the source chamber as a function of the distance relative to the front of the source nozzle, using the translation utility of the cascaded arc source. The n_0 has been determined by measuring the RS contribution in the mid part of the TS spectra. In an argon plasma, neutral density profiles could be measured with a spatial resolution of 2.2 mm and

2013 JINST 8 C11011

Table 1. TS system parameters.

Laser energy per pulse at the scattering volume	0.6 J
Typical measurement time (single pulse or multiple pulses at 10 Hz)	25 ns – 3 s
Solid angle at magnification $M = 0.267$ at viewing side.	6.2×10^{-3} sr
Length of scattering volume (corresponding to 24 CCD pixels)	2×10^{-3} m
Overall transmission from scattering volume to photocathode of ICCD	$\sim$ 0.2–0.26
Conversion efficiency counts per photoelectron (counts/photoelectron)	80
Spectral range/spectral resolution (400 μm slit, grating 3300 gr/mm)	10.2 nm/0.137 nm
Spectral range/spectral resolution (400 μm slit, grating 2670 gr/mm)	18 nm/0.24 nm
Spatial resolution (measured)	$<$ 2 mm
Density limit	1×10^{17} m^{-3}
Temperature limit	0.07 eV

an accuracy of 25% for $n_0 = 1.0 \times 10^{20}$ m^{-3}. The performance and the fact that the measured argon expansion properties, with $T_e < 0.15$ eV and $n_e < 3.0 \times 10^{19}$ m^{-3} (accuracy $\sim$ 3%), are in excellent agreement with the predictions, demonstrate that the TS system is not only an excellent diagnostic control tool for monitoring n_e, T_e and n_0 for Magnum-PSI, but also for detailed exploration of plasma phenomena. The specifications are listed in table 1.

3.1.1 Measurement of magnetized hydrogen plasma jet

TS was performed at a distance of 17 mm in front of a lithiated target. The viewing dump was absent to enable access for the fast IR and visible light camera observation.

Also in this case the detected stray light levels were negligible. In figures 4 and 5 n_e and T_e profiles are shown that were recorded with a repetition period of 2 s (accumulation duration 1 s, 10 pulses, spatial resolution 2 mm). In figure 6 a typical spectrum is shown.

3.1.2 Single pulse TS on the pulsed plasma

Using the ICCD in a higher hardware binning mode, a repetition rate of 5 Hz could be achieved enabling measurements of mimicked ELM pulses with single pulse TS. The pulsed source generated multiple identical ELM pulses with a time increment of 50 μs, each time relative to the TS pulse time. In this way TS could probe the pulse evolution (see figures 7 and 8). The repetition rate was limited due to the read-out speed of the camera: the CCD binning was increased to achieve this rate and therefore the spatial resolution was in this case 4 mm. These are unprecedented results, but can easily be obtained by using a programmable timing system.

3.2 Collective Thomson Scattering (CTS)

The ion temperature (T_i) and axial velocity ($\mathbf{v}_{\text{axial}}$) of the plasma are important parameters for the determination of the particle flux on plasma facing components that can be extracted from CTS [8]. For this type of scattering the size of the scattering wave is comparable to or greater than the Debye length of the plasma and the resulting narrow spectrum (the so-called ion feature) originates from scattering from the electrons bunched in the Debye sphere of the ions. From the spectral shape, the ratio between T_e (determined by incoherent TS) and T_i can be determined (see figure 9).

2013 JINST 8 C11011

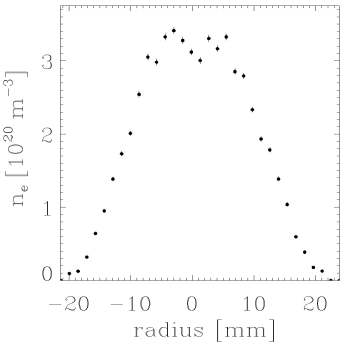

Figure 4. n_e profile plasma jet, measured at $\sim$ 17 mm distance from the target. Conditions: D_2 gas flow 7 Pa m^3/s, axial B field at source location 1.3 T, source current 175 A.

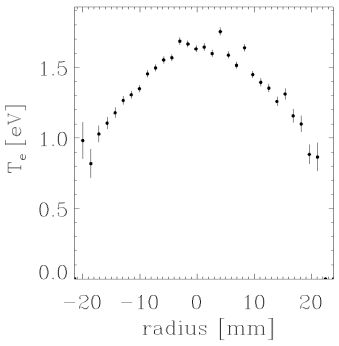

Figure 5. T_e profile plasma jet.

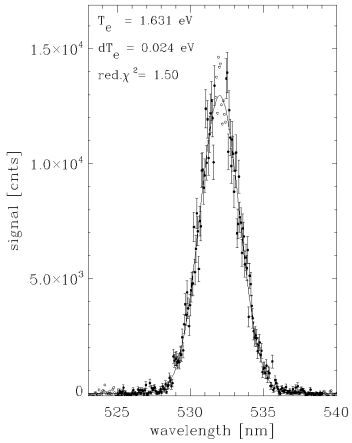

Figure 6. A typical spectrum, corresponding to r = 0 mm.

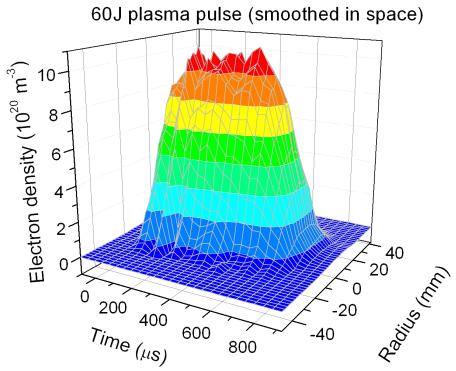

Figure 7. Time evolution of n_e profiles during ELM-like plasma pulse. Conditions: H_2gas flow 17 Pa m^3/s, axial B field at source location 1.3 T, source DC current 200 A and superposed pulsed current 550 A.

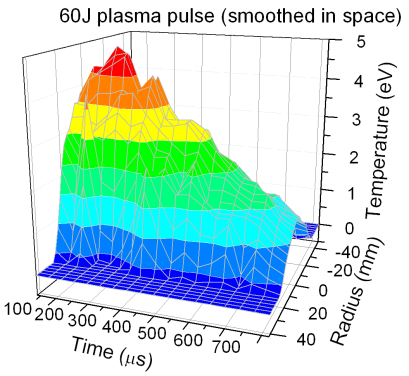

Figure 8. Time evolution of T_e profiles during ELM-like plasma pulse.

The Debye length of the Magnum-PSI plasma ($< 1\,\mu$m for high density) will be easily 100 times smaller than that of the bulk of a Tokamak plasma, i.e. the Magnum-PSI plasma conditions allows for good CTS performance at 1064 nm (detector compatible) and a scattering angle of about 30° (see figure 10).

The Doppler shift of the spectrum of the ion feature is a measure of the macroscopic velocity of the plasma, i.e. this property allows measurement of the radial and axial velocity of a plasma jet. In figure 11 a vector scheme is shown for the axial velocity measurement setup, i.e. only the velocity component ($\mathbf{v}_{\text{axial}} // \mathbf{B}$) with its projection on $\mathbf{k}$ is measured as a Doppler shift.

Implementation of CTS on Magnum-PSI is planned in 2014. Because, Magnum-PSI is being used intensively for different measurement campaigns, it was decided to perform CTS first in

2013 JINST 8 C11011

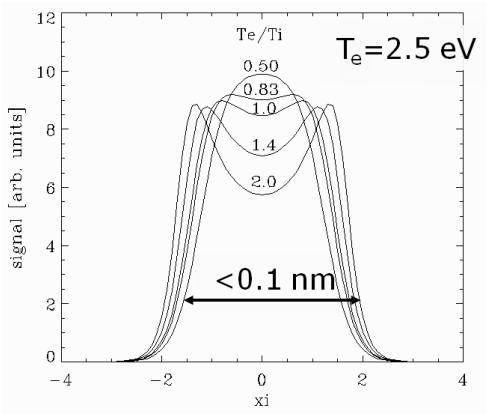

Figure 9. Calculated shape of the spectrum of the ion feature as a function of normalized wavelength for different values of T_e over T_i.

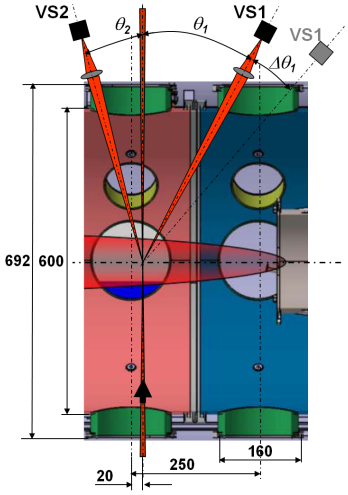

Figure 10. Side view of the CTS viewing system for Magnum. First tests will be performed at Pilot with about same (scattering angle 30°).

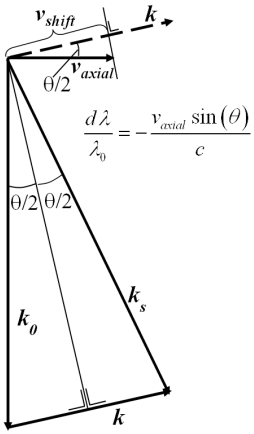

Figure 11. $\mathbf{v}_{\text{axial}}$ with its projection on k is measured as a Doppler shift $d\lambda$.

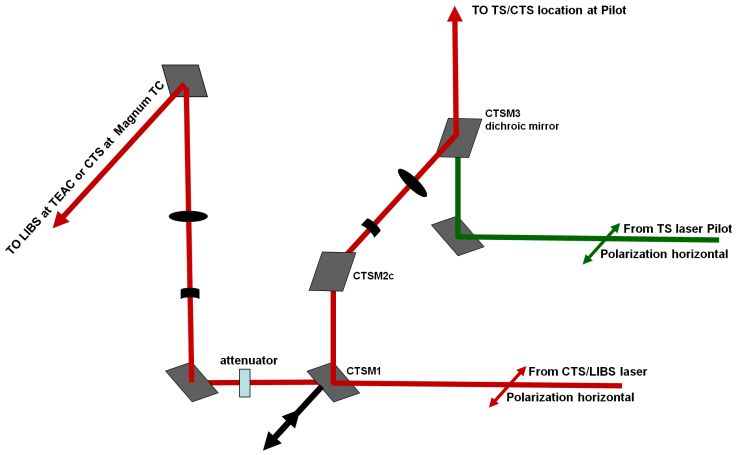

Figure 12. Laser beam divider, enabling TS and CTS at Pilot-PSI. By translating mirror CTSM1 CTS or LIBS can be performed in the TC or TEAC, respectively.

Pilot-PSI. First results are expected at the end of 2013. The construction of the laser beam line is almost finished: the 1064 nm laser beam is coupled in (using a dichroic mirror), such that the same trajectory as that of the incoherent TS system (532 nm, scattering angle 90°) [14] of Pilot (see figure 12) is followed. It consists of an advanced injection seeded laser Nd:YAG laser operating at the fundamental wavelength 1064 nm (linewidth 0.003 nm, 1.3 J/pulse, 10 Hz, pulse width (FWHM $\sim$ 7 ns)).

Two methods of detection are being realized to permit mutual verification of the extremely narrow TS spectra ($<$ 0.1 nm). A Fabry Perot etalon setup is being built (see figure 13) that enables scanning over its free spectral range by tilting the etalon, i.e. it acts as a narrow band pass filter with variable central wavelength. In combination with one APD (Avalanche Photodiode, effective

2013 JINST 8 C11011

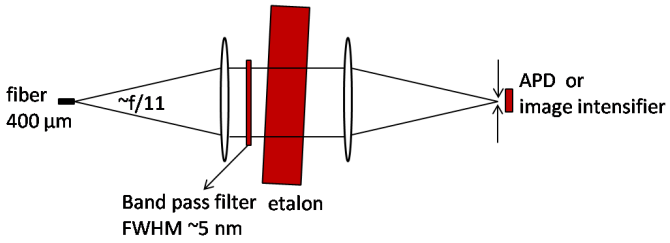

Figure 13. Fabry Perot interferometer.

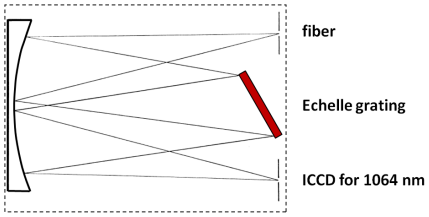

Figure 14. Ebert spectrometer.

quantum efficiency (QE) $\sim$ 20% at 1064 nm) CTS spectra can be recorded for one spatial point. For each angular step, corresponding to $\sim$ 0.006 nm shift of the pass band of etalon, a number of laser shots have to be performed to achieve good statistics, i.e. to obtain a full spectrum this has to be repeated till the required spectral range is scanned. To achieve a spectral resolution of 0.006 nm the etalon setup requires that the input beam exhibit a full angle divergence of about 3.5 mrad. This is achieved by using a viewing f-numbers of 1/30 and magnification $M = -0.4$. The light cone, with f-number 1/12, radiated by the 400 um fiber results in a 10 mm diameter parallel beam after the input lens (f$\sim$ 114 mm). The acceptance angle of etalon system maps very well with that of the viewing system.

A very high resolution ($\sim$ 0.004 nm at slit width 50 μm) Echelle spectrometer (HRES) (f/11, 1.5 m) (see figure 14) will be built that is equipped with the only currently commercially available image intensifier (Katod, Russia) that exhibits NIR sensitivity around 1064 nm combined with a low noise CCD (Princeton Instruments PIXIS). Although the QE of the image intensifier is only 1% at 1064 nm, accumulation of the data will allow to obtain the TS signal (2–4 seconds). This allows for imaging CTS, i.e. measuring ion temperature profiles. However, because we will initially only use one detection fiber, the T_i of one spatial point in the plasma can be measured. In table 2 the most important system parameters are summarized. The 400 μm diameter fiber (35 m long) is made compatible with the narrow input of the spectrometer by converting the fiber core to a strip of 64 μm diameter fibers.

3.2.1 Expected performance

According to [8] the expected number of photoelectrons (pe) can be calculated. Using table 2 as a guide, it is found that for the FPI setup for n_e between 2.0–4.0$\times 10^{21}$ m^{-3} about 22800–65500 pe can be expected. As the APD will collect only a part of the spectrum (FWHM 0.006 nm), for the low density range for good statistics and noise reduction (APD's exhibit noise levels in the range of < 90 pe) signal averaging has to be applied for $\sim$ 5 laser pulses. To form one full spectrum about 20 spectral measurement points have to be obtained, i.e. a full spectrum can be obtained in about 10 s.

In table 2 it can be seen that for the HIRES spectrometer the expected number of photoelectrons accumulated during 30 laser pulses (3 s), is such that for n_e between 1.3–4.0$\times 10^{21}$ m^{-3} the ion temperature can be determined with an accuracy of 10%. For measuring ion temperature profiles a spectrometer is most suited, but a more advanced Fabry Perot interferometer (SLS Optics) can be used to resolve extremely narrow spectra for the observation of small Doppler shifts (or the temperature of heavier masses [8]).

2013 JINST 8 C11011

Table 2. Main parameters of the prototype collective TS system based on a Fabry Perot interferometer and HIRES spectrometer detection: test case $T_e = 2.5$ eV.

CTS using two detection schemes:	**FPI**	**HRES**	**Units**
Scattering angle	30	30	$^\circ$
Accumulated number of laser pulses at 10 Hz (1.1 J/pulse)	5×20	30	pulses
Length scattering volume (L)	1.5	1.5	mm
Solid angle ($f/30$) (Ω)	0.87×10^{-3}	0.87×10^{-3}	sr
Overall transmission up to detector (τ_{overal})	45	30	%
Effective quantum efficiency	20	1	%
Width spectrometer input (fibre diameter)	400 60	64	μm
Optical spectral resolution	0.006	~ 0.004	nm
Chosen n_e range (lower n_e range at scattering angle $< 30^\circ$)	2.0–4.0	1.3–4.0	10^{21} m^{-3}
α range	1.25–1.76	1.0–1.76	
Relative spectral imprecision $d\lambda^i_{rel}$*	2.2	2.2	%
Relative ion feature contribution ($S_i(k)$)	23–33	17–33	%
Full 1/e-width spectrum	0.08	0.08	nm
Number of photoelectrons [8]	22.8–65.5	1.1–6.5	10^3 pe

* The imprecision $d\alpha$ is caused by the fact that TS requires a cone collection angle (around θ, see figure 10) , this means that scattered light is collected over a cone of **k** vectors, i.e. the observed spectrum will consist of contributions originating from all the **k**'s within this cone [8].

It is expected that the axial velocity of the bulk of the plasma column will range from 3–10 km/s [15]. According to [8] this corresponds to a Doppler shift range of 0.0063–0.018 nm. Using the HIRES spectrometer the observational error in the velocity determination is expected to be about 15% at a velocity of 3000 m/s and better for higher velocities [8]. To observe the rotation of the plasma beam, the scattering plane of the CTS system has to be directed perpendicularly to the plasma beam direction. Rayleigh scattering will be used for determining the non-Doppler shifted reference spectrum.

3.3 Laser Induced Breakdown Spectroscopy (LIBS)

A LIBS diagnostic is operational and is used to measure elemental depth profiles and composition of the superficial layers of samples. The LIBS system can be used for targets located inside the TEAC ($\sim$ 34 m distance from LIBS laser) (see figure 15) before and after plasma exposure (without exposing them to atmosphere) and for targets located in a neighbouring room close to the laser room for post mortem measurements.

In principle deuterium retention can be measured, but whether LIBS can be used for quantitative detection of deuterium, is still a subject of research and is outside the scope of this paper. It is observed that at laser energy densities in the range of 30 J/cm^2 the intensity of the obtained spectra as well as the ablation rate of $\sim$ 130 nm/pulse is reproducible. In table 3 several features and typical specifications are summarized.

An advantage to the use of this LIBS system is the fact that the detection window can be delayed such that continuum radiation and Stark broadening is reduced: this leads to good sig-

2013 JINST 8 C11011

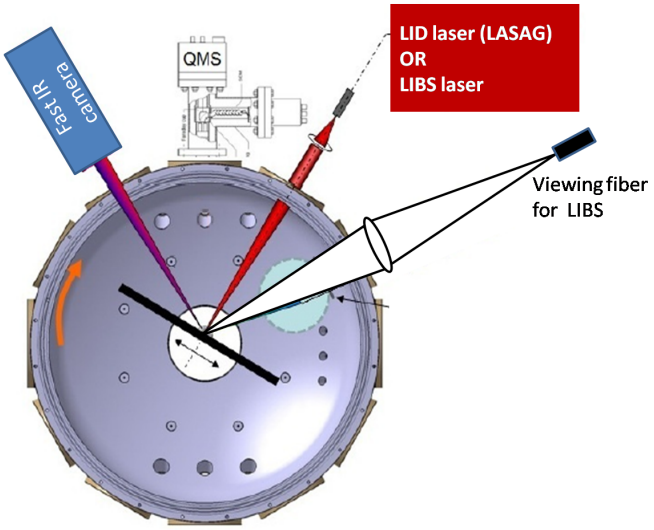

Figure 15. Top view of TEAC. LIBS and LID-QMS laser injection system and IR camera (required for laser spot temperature measurements during LID) are shown here. To enable LIBS measurements the conventional laser beam is implemented by switching a mirror. The light from the resulting LIBS plume is collected by a viewing system.

Table 3. LIBS system parameters.

Nd:YAG Powerlite Precision II 8000, 1064 nm (FWHM $\sim$ 7 ns, 10 Hz) operated at	0.2 J/pulse
Spot diameter 0.9 mm giving energy density:	~ 30 J/cm^2
Effective viewing f-number: $\sim 1/10$; solid angle	7.8×10^{-3} sr
Detection fiber (length 40 m) (single fiber)	UV 800/880
Fiber convertor from Fiberware GmbH: 120 (AS 64/70 IR PI 7) fibers arranged in a circle of 800 μm converted to a line of $\sim$ 8 mm heights to adapt to spectrometer input. Current system convertor with 50 μm fibers, fill factor $< 40\%$)	70%
Spectral range currently	60 nm
Spectrometer fiber width 64 μm, spectral resolution (7 pixels), grating 300 gr/mm	0.31 nm
Observation area (fiber core 0.8 mm, magnification about 1)	0.8×10^{-3} m
Used gate width detection window:	400–800 ns
Vessel pressure:	5×10^{-5} Pa

nal/(plasma light) ratios and clear identification of the different lines. A disadvantage of the existing detection system is the short spectral range of $\sim$ 60 nm compared to that of a wide range Echelle spectrometer. However the current configuration with effective fiber coupling to the spectrometer enables more light to be collected compared to Echelle spectrometers.

In figures 16 and 17 a typical LIBS measurement, performed at short distance from the laser, is shown. Here the target was composed of a 3 μm layer of diamond like carbon on a tungsten

2013 JINST 8 C11011

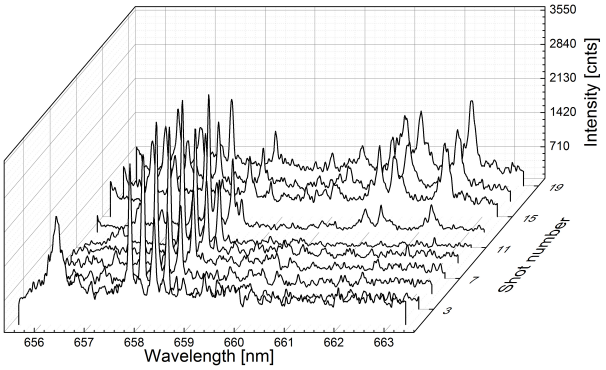

Figure 16. LIBS: spectra shown as function of shot number. Wavelength range 655 nm – 663 nm. Delay time gate window relative to laser pulse 400 ns.

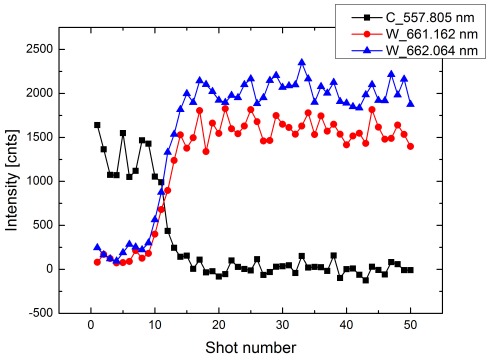

Figure 17. Maximum value of W and C lines as function of shot number.

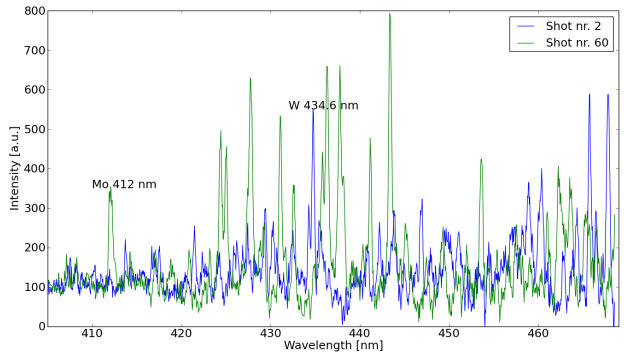

Figure 18. LIBS spectra for laser shot number 2 and 60. It can be seen that the W lines has disappeared at shot 60, while the Mo line has appeared. The background originates from the continuum and is significant due to the fact that the delay time of the detection window was short (in the range of 100 ns) relative to laser pulse.

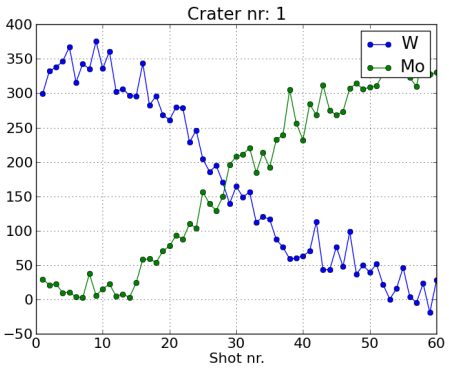

Figure 19. Maximum value of W (434.7 nm) and Mo line (412.01 nm) as function of shot number. After 10–15 shots the Mo layer is reached. Wavelength range 405–470 nm.

substrate The transition from carbon to tungsten is clearly visible in figure 17; penetration depth about 200 nm/shot (spot size $\sim$ 1.7 mm).

In figures 18 and 19 a measurement performed in the TEAC (long beam line) is presented. The target consisted of a 2 μm tungsten layer on a thick molybdenum substrate. A transition from carbon to molybdenum is also in this case clearly visible; the penetration depth is in this case in the range of 130 nm/shot (spot size $\sim$ 0.9 mm). The signal levels and the shapes of depth profiles may be improved by using a fiber convertor with better transmission as well as optimization of the laser beam profile. In figure 19 relative high amplitude fluctuations are visible. This is probably caused by the fact that at the time of measurements some components of the laser beam were not thoroughly mounted; vibrations of the beam line could cause ablation of neighbouring material during the scan.

2013 JINST 8 C11011

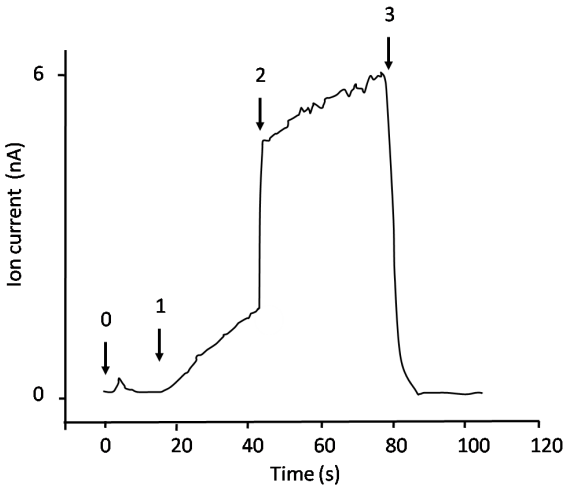

Figure 20. LID-QMS measurement according to upper schema: D (mass 4) ion current. After the QMS is started (0), the valve between turbo pump and TEAC vessel is closed (1). A sharp increase D signal is observed when the laser is fired (2), indicating D desorption. The linear signal increase (starting from (1)) before the shot represents the background. At (3) the valve is opened.

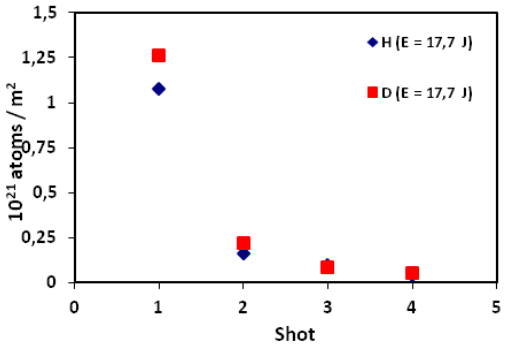

Figure 21. LID-QMS measurement on a target with a certain D content. D concentration for four subsequent shots. The main contribution for H and D comes from mass 3 (HD) and 4 (D_2) and 2 (H_2).

3.4 Laser induced desorption combined with quadrupole mass spectroscopy (LID-QMS)

Laser induced desorption has been implemented in the TEAC (see figure 15) for determination of deuterium retention in plasma exposed samples. A pulsed LASAG laser with a fiber based beam line is located in the laser room and the output of the fiber is imaged to a spot size of $\sim$ 2–3 mm on the target, enabling heating to a temperature $>$ 1400 K such that desorption of impurities inside the material occurs. The amount of released deuterium is determined by a very sensitive high resolution quadrupole mass spectrometer. During the experiments, the valve between turbo pump and vessel is closed and the background pressure is in the range of 10^{-5} Pa.

The steps taken in a typical LID-QMS experiment are shown in figure 20, together with the ion current of the QMS set to mass 4. After the measurement procedure it takes around 5 minutes to restore the background pressure of the vessel (10^{-5} Pa). When the pressure is stabilized another measurement can be performed. This procedure is repeated three times at each location to make sure that most of the deuterium is desorbed. The absolute sensitivity of the QMS system is determined by using a calibrated deuterium leak. In figure 21 a typical example of a LID-QMS measurement is shown.

It is required that the amount of retained deuterium can be determined locally and quantitatively: this permits the determination of spatially localised retention profiles over the surface of an exposed target.

However, the amount of deuterium that will be desorbed in LID depends on the depth to which the deuterium has diffused and on the energy with which it is trapped. In the case that the implantation depth is the same over the whole surface (and assuming homogeneous material

2013 JINST 8 C11011

structure), a reliable retention profile can be measured. Not all deuterium may be desorbed in the LID experiment, but the absolute retention can be determined by normalization to results from thermal desorption spectroscopy. Nevertheless, LID-QMS data need to be interpreted carefully.

4 Summary and conclusions

The advanced Thomson Scattering system built for the linear plasma generator Magnum-PSI is operational.

Very low n_e ($9 \times 10^{18}\,m^{-3}$) can be measured within seconds with accuracies better than 6%. The minimum measurable electron density and temperature are $n_e < 1 \times 10^{17}\,m^{-3}$ and $T_e \sim 0.07\,eV$, respectively. By virtue of the high system sensitivity, single pulse TS (repetition period 200 ms) can be performed on high density pulsed plasmas giving unparalleled results.

A CTS system is being built for measuring the ion temperature and macroscopic velocity of the plasma. The design is ready and the tryout of a prototype of the system will be performed first at Pilot-PSI, first results expected in 2013.

A LIBS system is operational at Magnum-PSI. Elemental depth profiles can be extracted from the first measurements. Improvements are being implemented.

LID-QMS is used regularly at Magnum-PSI. Quantitative deuterium retention profiles are obtained by normalization to the total retention determined by TDS.

Acknowledgments

The authors wish to thank especially the people from the workshop, design office and Electronics & ICT departments of the FOM Institute for Plasma Physics Rijnhuizen for their wonderful support. This work, supported by the European Communities under the contract of the Association EURATOM/FOM, was carried out within the framework of the European Fusion Programme with financial support from NWO and the Centre-of-Excellence on Fusion Physics and Technology (NWO-RFBR grant 047.018.002). The views and opinions expressed herein do not necessarily reflect those of the European Commission.

References

[1] www.iter.org.

[2] J. Rapp et al. *Construction of the plasma-wall experiment Magnum-PSI*, *Fusion Eng. Des.* **85** (2010) 1455.

[3] M.J. de Graaf, R. Severens, R.P. Dahiya, M.C.M. van de Sanden and D.C. Schram, *Anomalous fast recombination in hydrogen plasmas involving rovibrational excitation*, *Phys. Rev.* **E 48** (1993) 2098.

[4] G.J. van Rooij et al., *Extreme hydrogen plasma densities achieved in a linear plasma generator*, *Appl. Phys. Lett.* **90** (2007) 121501.

[5] G. De Temmerman, J.J. Zielinski, H.J. van der Meiden, W . Melissen and J. Rapp, *Production of high transient heat and particle fluxes in a linear plasma device*, *Appl. Phys. Lett.* **97** (2010) 081502.

2013 JINST 8 C11011

[6] H.J.N. van Eck, T.A.R. Hansen, A.W. Kleyn, H.J. van der Meiden, D.C. Schram and P.A. Zeijlmans van Emmichoven, *A differentially pumped argon plasma in the linear plasma generator Magnum-PSI: gas flow and dynamics of the ionized fraction Plasma Sources Sci. Technol.* **20** (2011) 045016.

[7] H.J. van der Meiden et al., *Advanced Thomson scattering system for high-flux linear plasma generator*, *Rev. Sci. Instrum.* **83** (2012) 123505.

[8] H.J. van der Meiden, *Collective Thomson scattering for ion temperature and velocity measurements on Magnum-PSI: a feasibility study*, *Plasma Phys. Control. Fusion* **52** (2010) 045009.

[9] V.P. Veremiyenko, *An ITER-relevant Magnetized Hydrogen Plasma Jet*, Ph.D thesis, Eindhoven University of Technology, Netherlands (2006).

[10] B. Schweer, F. Irrek, G. Sergienko, V. Philipps and U. Samm, *In situ diagnostic for monitoring of deuterium and tritium in re-deposited carbon layers by laser induced desorption*, *J. Nucl Mater.* **363–365** (2007) 1375.

[11] V. Philipps et al., *Development of laser-based techniques for in situ characterization of the first wall in ITER and future fusion devices*, *Nucl. Fusion* **53** (2013) 093002.

[12] N.N Naumenko and S.N. Tugarinov, workshop *Active Beam Spectroscopy for control of the fusion plasma*, Lorentz Center, Leiden, The Netherlands (2009).

[13] M.C.M. van de Sanden, J.M. de Regt and D.C. Schram, *Recombination of argon in an expanding plasma jet*, *Phys. Rev.* **E 47** (1993) 2792.

[14] H.J. van der Meiden et al., *High sensitivity imaging Thomson scattering for low temperature plasma*, *Rev. Sci. Instrum.* **79** (2008) 013505-1/8.

[15] A.E. Shumack et al., *Rotation of a strongly magnetized hydrogen plasma column determined from an asymmetric Balmer-beta spectral line with two radiating distributions*, *Phys. Rev.* **E 78** (2008) 046405.

2013 JINST 8 C11011